RSC Advances

PAPER

View Article Online
View Journal | View Issue

Cite this: *RSC Adv.*, 2017, **7**, 20582

Synthesis and biological evaluation of novel technetium-99m-labeled phenylquinoxaline derivatives as single photon emission computed tomography imaging probes targeting β-amyloid plaques in Alzheimer's disease†

Shimpei Iikuni, Masahiro Ono,* Keiichi Tanimura, Hiroyuki Watanabe, Masashi Yoshimura and Hideo Saji

The development of an imaging probe targeting β-amyloid (Aβ) plaques in Alzheimer's disease labeled with technetium-99m, the most commonly used radioisotope for clinical diagnoses, has been strongly anticipated. In this study, we synthesized three novel ^{99m}Tc complexes with the phenylquinoxaline scaffold and evaluated their properties for imaging Aβ plaques. The ^{99m}Tc and corresponding Re complexes were synthesized with bis(aminoethanethiol) (BAT) as a chelating ligand. In a binding affinity assay using recombinant Aβ(1–42) aggregates *in vitro*, the ^{99m}Tc-labeled *N*,*N*-dimethylated phenylquinoxaline derivative (^{99m}Tc-BAT-C3-PQ-1) and the corresponding Re complex showed sufficient affinity for Aβ(1–42) aggregates. An *in vivo* biodistribution study in normal mice revealed that ^{99m}Tc-BAT-C3-PQ-1 showed a moderate initial brain uptake and a reasonable clearance from the brain. An *ex vivo* autoradiographic examination with ^{99m}Tc-BAT-C3-PQ-1 showed the marked labeling of Aβ plaques in brain sections from Tg2576 transgenic mice but not age-matched controls. ^{99m}Tc-BAT-C3-PQ-1 may be a potential single photon emission computed tomography probe for imaging Aβ plaques in Alzheimer's disease.

Received 19th December 2016
Accepted 31st March 2017

DOI: 10.1039/c6ra28395k

rsc.li/rsc-advances

Introduction

Alzheimer's disease (AD) is the most common neurodegenerative disorder of the brain, with symptoms of memory loss, continuous cognitive decline, and behavioral disturbance. AD is pathologically characterized by the extracellular deposition of senile plaques consisting of β-amyloid (Aβ) and the intracellular deposition of neurofibrillary tangles consisting of hyperphosphorylated tau. AD is responsible for 60–70% of dementia in the elderly.[1,2] Currently, there is no medical treatment that cures or prevents AD.[1] Since Aβ deposition is believed to play a key role in neurodegeneration and begin prior to the onset of the disease, the development of an Aβ-targeted drug for AD has attracted much interest.[3] The early diagnosis of AD will be needed for early intervention and appropriate treatment of the disease.

Nuclear medical diagnoses with positron emission tomography (PET) have been utilized as major *in vivo* imaging modalities to carry out noninvasive diagnosis. Over the past few decades, research on the imaging of Aβ aggregates in AD brains with PET has made marked progress. Many clinical studies using [^{11}C]PIB, which is the main Aβ imaging probe, have proved this utility for AD diagnosis.[4–7] More recently, [^{18}F]florbetapir (Amyvid),[7–9] [^{18}F]flutemetamol (Vizamyl),[4,10,11] and [^{18}F]florbetaben (Neuraceq)[7,12,13] have been approved by the U.S. Food and Drug Administration for clinical AD diagnosis. However, the routine clinical use of PET probes labeled with ^{11}C and ^{18}F might be limited by their short physical half-lives ($t_{1/2}$ = 20 and 110 min, respectively).

To address the problem of an increase in AD patients in the world, more generally versatile Aβ imaging with single photon emission computed tomography (SPECT) is needed. In exploratory research on the development of Aβ imaging probes for SPECT, a number of radioiodinated compounds with affinity for Aβ aggregates have been reported.[14–17] Among them, a recent report suggested that [^{123}I]ABC577 may be a clinically useful tracer for SPECT imaging of Aβ plaques in the brains of AD patients.[18]

Among clinically utilized radioisotopes for SPECT, ^{99m}Tc is the most commonly used in nuclear medical diagnoses for several reasons, including easy production by a ^{99}Mo/^{99m}Tc generator, its physical half-life (6.01 h) being compatible with

Department of Patho-Functional Bioanalysis, Graduate School of Pharmaceutical Sciences, Kyoto University, 46-29 Yoshida Shimoadachi-cho, Sakyo-ku, Kyoto 606-8501, Japan. E-mail: ono@pharm.kyoto-u.ac.jp; Fax: +81-75-753-4568; Tel: +81-75-753-4608

† Electronic supplementary information (ESI) available. See DOI: 10.1039/c6ra28395k

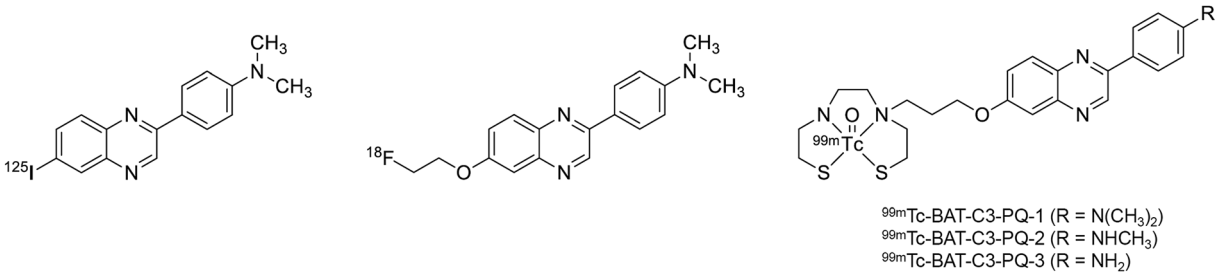

Fig. 1 Chemical structures of the radioiodinated or radiofluorinated phenylquinoxaline derivatives reported in our previous study, and ^{99m}Tc-labeled phenylquinoxaline derivatives in the present study.

the biological localization, and its γ-ray energy (141 keV) suitable for *in vivo* imaging. Thus, the development of ^{99m}Tc-labeled Aβ imaging probes will provide simple, convenient, and widespread SPECT-based imaging methods for the detection of Aβ plaques in the living brain.

To develop useful ^{99m}Tc-labeled imaging agents targeting Aβ depositions in AD brains, compact and neutral ^{99m}Tc-labeled ligands have been reported, such as derivatives of biphenyl,[19] phenylbenzothiazole,[20] chalcone,[21] flavone, aurone,[22] curcumin,[23] arylbenzofuran,[24,25] dibenzylideneacetone,[26] and arylbenzoxazole.[27,28] However, there have been no reports on the development of clinically useful ^{99m}Tc-labeled probes due to either low affinity for Aβ aggregates or low brain uptake.

We previously reported phenylquinoxaline derivatives labeled with ^{125}I or ^{18}F targeting Aβ in AD brains (Fig. 1).[29–31] These derivatives displayed high binding affinity for Aβ aggregates with K_i values in the nM range and showed specific labeling of Aβ plaques in sections of brain tissue from AD patients. Notably, [^{18}F]PQ-6 showed an excellent K_i value (0.895 nM) and intensive specific labeling of Aβ in the AD brain section.[30] These properties were superior to those of clinically used Aβ imaging probes, such as [^{11}C]PIB and [^{18}F]florbetapir (K_i = 9.00 and 12.8 nM, respectively). Based on these encouraging results, we designed novel ^{99m}Tc-labeled Aβ imaging probes with the scaffold of phenylquinoxaline (Fig. 1). Unlike radiohalogens, a chelating ligand is necessary for the introduction of metal ^{99m}Tc to the organic molecule. Considering the permeability at the blood–brain barrier (BBB), we selected bis(aminoethanethiol) (BAT) as a compact chelating ligand to form a neutral ^{99m}Tc complex. We herein synthesized novel ^{99m}Tc complexes based on phenylquinoxaline with BAT and evaluated their biological properties as potential SPECT probes targeting Aβ plaques in AD.

Materials and methods

General

All reagents were obtained commercially and used without further purification unless otherwise indicated. Na^{99m}TcO$_4$ was purchased from Nihon Medi-Physics Co., Ltd. (Tokyo, Japan) or obtained from a commercial ^{99}Mo/^{99m}Tc generator (Ultra-Techne Kow; FUJIFILM RI Pharma Co., Ltd., Tokyo, Japan). W-Prep 2XY (Yamazen, Osaka, Japan) was used for silica gel column chromatography on a Hi Flash silica gel column (40 μm, 60 Å, Yamazen). ^{1}H NMR spectra were recorded on a JNM-ECS400 (JEOL, Tokyo, Japan) with tetramethylsilane (TMS) as an internal standard. Coupling constants are reported in Hertz. Multiplicity was defined as singlet (s), doublet (d), triplet (t), or multiplet (m). Mass spectra were obtained on a SHIMADZU LCMS-2020 EV (SHIMADZU, Kyoto, Japan). High-resolution mass spectrometry (HRMS) was conducted with a LCMS-IT-TOF (SHIMADZU). Reversed-phase high-performance liquid chromatography (RP-HPLC) was performed with a Shimadzu system (SHIMADZU, an LC-20AT pump with an SPD-20A UV detector, λ = 254 nm) with a Cosmosil C_{18} column (Nacalai Tesque, Kyoto, Japan, 5C_{18}-AR-II, 4.6 × 150 mm) delivered at a flow rate of 1.0 mL min^{-1} using a solvent of H_2O/MeCN [11 : 9 (0 min) to 1 : 3 (30 min)] as the mobile phase.

Animals

Animal experiments were conducted in accordance with our institutional guidelines and were approved by the Kyoto University Animal Care Committee. Male ddY mice were purchased from Japan SLC, Inc. (Shizuoka, Japan). Female Tg2576 and wild-type mice were purchased from Taconic Farms, Inc. (New York, U.S.A.). Animals were fed standard chow and had free access to water. All efforts were made to minimize suffering.

Chemistry

Synthesis of *N*-methyl-4-(4,4,5,5-tetramethyl-1,3,2-dioxaborolan-2-yl)aniline (1). To a suspension of 4-(4,4,5,5-tetramethyl-1,3,2-dioxaborolan-2-yl)aniline (1.10 g, 5.0 mmol) and paraformaldehyde (901 mg, 30 mmol) in MeOH (10 mL) was slowly added sodium methoxide (5 M in MeOH, 4.0 mL, 20 mmol). The mixture was heated to reflux for 1 h and then allowed to cool to 0 °C. $NaBH_4$ (946 mg, 25 mmol) was added gently. The reaction mixture was brought to reflux again for 1.5 h and then quenched with saturated $NaHCO_3$ (aq.). After the addition of H_2O (50 mL), the mixture was extracted with $CHCl_3$ (50 mL × 2). The organic phases were combined and dried over $MgSO_4$. Evaporation of the solvent afforded a residue, which was purified by silica gel chromatography (AcOEt/hexane = 1 : 5) to give 302 mg of **1** (26%). ^{1}H NMR (400 MHz, $CDCl_3$) δ 7.55 (d, J = 6.8 Hz, 2H), 6.45 (d, J = 6.8 Hz, 2H), 3.86 (s, broad, 1H), 2.69 (s, 3H), 1.21 (s, 12H). MS (ESI): m/z calculated for $C_{13}H_{21}BNO_2^+$ [M + H]$^+$, 234; found, 234.

Synthesis of *tert*-butyl(2-((3-bromopropyl)(2-(tritylthio)ethyl)amino)ethyl)(2-(tritylthio)ethyl)carbamate (2). A solution of Trt-Boc-BAT (1.53 g, 2.0 mmol), 1,3-dibromopropane (223 μL, 2.2 mmol), *N*,*N*-diisopropylethylamine (697 μL, 4.0 mmol) in dimethylformamide (DMF) (5 mL) was stirred at 90 °C for 3 h. After cooling to room temperature, the mixture was concentrated. The residue was purified by silica gel chromatography (AcOEt/hexane = 1 : 5) to give 454 mg of **2** (26%). ^{1}H NMR (400 MHz, $CDCl_3$) δ 7.41–7.39 (m, 12H), 7.29–7.23 (m, 12H), 7.22–7.17 (m, 6H), 3.32 (s, 2H), 3.00–2.82 (m, 4H), 2.38–2.16 (m, 10H), 1.76–1.70 (m, 2H), 1.37 (s, 9H). MS (ESI): *m*/*z* calculated for $C_{52}H_{58}BrN_2O_2S_2^+$ $[M + H]^+$, 887; found, 887.

Synthesis of 2-chloroquinoxalin-6-ol (3). Compound **3** was synthesized from 2-chloro-6-methoxyquinoxaline according to a previous report.[30]

Synthesis of 2-(4-(dimethylamino)phenyl)quinoxalin-6-ol (4). To a solution of **3** (181 mg, 1.0 mmol) and *N*,*N*-dimethyl-4-(4,4,5,5-tetramethyl-1,3,2-dioxaborolan-2-yl)aniline (272 mg, 1.1 mmol) in 2 M Na_2CO_3 (aq.)/dioxane (1 : 1, 16 mL) was added $Pd(PPh_3)_4$ (115 mg, 0.10 mmol). The mixture was heated to reflux for 1 h. After cooling to room temperature, H_2O (50 mL) was added. After the extraction of the mixture with AcOEt (50 mL × 2), the organic phases were combined and dried over $MgSO_4$. Evaporation of the solvent afforded a residue, which was purified by silica gel chromatography ($CHCl_3$/MeOH = 10 : 1) to give 236 mg of **4** (89%). ^{1}H NMR (400 MHz, DMSO-d_6) δ 9.31 (s, 1H), 8.13 (d, J = 7.6 Hz, 2H), 7.87 (d, J = 8.4 Hz, 1H), 7.35 (d, J = 8.4 Hz, 1H), 7.23 (s, 1H), 6.86 (d, J = 7.6 Hz, 2H), 3.01 (s, 6H). MS (ESI): *m*/*z* calculated for $C_{16}H_{16}N_3O^+$ $[M + H]^+$, 266; found, 266.

Synthesis of 2-(4-(methylamino)phenyl)quinoxalin-6-ol (5). To a solution of **3** (181 mg, 1.0 mmol) and **1** (256 mg, 1.1 mmol) in 2 M Na_2CO_3 (aq.)/dioxane (1 : 2, 30 mL) was added $Pd(PPh_3)_4$ (115 mg, 0.10 mmol). The mixture was heated to reflux for 30 min. After cooling to room temperature, H_2O (200 mL) was added. The mixture was extracted with AcOEt (100 mL × 2). The organic phases were combined and dried over $MgSO_4$. Evaporation of the solvent afforded a residue, which was purified by silica gel chromatography (AcOEt/hexane = 1 : 1) to give 153 mg of **5** (61%). ^{1}H NMR (400 MHz, $CDCl_3$) δ 9.06 (s, 1H), 7.98 (d, J = 8.8 Hz, 2H), 7.90 (d, J = 9.2 Hz, 1H), 7.37 (s, 1H), 7.33–7.29 (m, 1H), 6.70 (d, J = 8.8 Hz, 2H), 2.90 (s, 3H). MS (ESI): *m*/*z* calculated for $C_{15}H_{14}N_3O^+$ $[M + H]^+$, 252; found, 252.

Synthesis of 2-(4-aminophenyl)quinoxalin-6-ol (6). To a solution of **3** (361 mg, 2.0 mmol) and 4-(4,4,5,5-tetramethyl-1,3,2-dioxaborolan-2-yl)aniline (482 mg, 2.2 mmol) in 2 M Na_2CO_3 (aq.)/dioxane (1 : 1, 24 mL) was added $Pd(PPh_3)_4$ (231 mg, 0.20 mmol). The mixture was heated to reflux for 2 h. After cooling to room temperature, H_2O (60 mL) was added. The mixture was extracted with AcOEt (60 mL × 2). The organic phases were combined and dried over $MgSO_4$. Evaporation of the solvent afforded a residue, which was purified by silica gel chromatography (AcOEt/hexane = 3 : 1) to give 49 mg of **6** (10%). ^{1}H NMR (400 MHz, CD_3OD) δ 9.14 (s, 1H), 7.94 (d, J = 8.8 Hz, 2H), 7.91 (d, J = 9.2 Hz, 1H), 7.37 (dd, J = 9.2, 2.8 Hz, 1H), 7.26 (d, J = 2.8 Hz, 1H), 6.83 (d, J = 8.8 Hz, 2H). MS (ESI): *m*/*z* calculated for $C_{14}H_{12}N_3O^+$ $[M + H]^+$, 238; found, 238.

Synthesis of *tert*-butyl(2-((3-((2-(4-(dimethylamino)phenyl)quinoxalin-6-yl)oxy)propyl)(2-(tritylthio)ethyl)amino)ethyl)(2-(tritylthio)ethyl)carbamate (7). A solution of **2** (100 mg, 0.11 mmol), **4** (73 mg, 0.26 mmol), and cesium carbonate (171 mg, 0.52 mmol) in DMF (5 mL) was stirred at 70 °C for 2 h. After being neutralized with saturated NH_4Cl (aq.), the mixture was extracted with $CHCl_3$ (50 mL × 2). The organic phases were combined and dried over $MgSO_4$. After being evaporated to dryness, the residue was purified by silica gel chromatography (AcOEt/hexane = 1 : 1) to give 87 mg of **7** (62%). ^{1}H NMR (400 MHz, $CDCl_3$) δ 9.18 (s, 1H), 8.09 (d, J = 8.8 Hz, 2H), 7.92 (d, J = 9.2 Hz, 1H), 7.40–7.37 (m, 14H), 7.30–7.27 (m, 6H), 7.23–7.16 (m, 12H), 6.85 (d, J = 8.8 Hz, 2H), 4.03 (t, J = 6.0 Hz, 2H), 3.07 (s, 6H), 2.95–2.84 (m, 4H), 2.41–2.25 (m, 10H), 1.76 (t, J = 6.4 Hz, 2H), 1.37 (s, 9H). MS (ESI): *m*/*z* calculated for $C_{68}H_{72}N_5O_3S_2^+$ $[M + H]^+$, 1070; found, 1070.

Synthesis of *tert*-butyl(2-((3-((2-(4-(methylamino)phenyl)quinoxalin-6-yl)oxy)propyl)(2-(tritylthio)ethyl)amino)ethyl)(2-(tritylthio)ethyl)carbamate (8). A solution of **2** (100 mg, 0.11 mmol), **5** (66 mg, 0.26 mmol), and cesium carbonate (171 mg, 0.52 mmol) in DMF (5 mL) was stirred at 70 °C for 30 min. After being neutralized with saturated NH_4Cl (aq.), the mixture was extracted with $CHCl_3$ (50 mL × 2). The organic phases were combined and dried over $MgSO_4$. After being evaporated to dryness, the residue was purified by silica gel chromatography (AcOEt/hexane = 1 : 1) to give 38 mg of **8** (27%). ^{1}H NMR (400 MHz, $CDCl_3$) δ 9.17 (s, 1H), 8.05 (d, J = 8.4 Hz, 2H), 7.92 (d, J = 8.8 Hz, 1H), 7.40–7.37 (m, 12H), 7.30–7.28 (m, 6H), 7.23–7.16 (m, 14H), 6.74 (d, J = 8.4 Hz, 2H), 4.03 (t, J = 6.4 Hz, 2H), 3.02–2.96 (m, 2H), 2.92 (s, 3H), 2.42–2.25 (m, 12H), 1.77 (t, J = 6.4 Hz, 2H), 1.37 (s, 9H). MS (ESI): *m*/*z* calculated for $C_{67}H_{70}N_5O_3S_2^+$ $[M + H]^+$, 1056; found, 1056.

Synthesis of Re-BAT-C3-PQ-1 (9). To a solution of **7** (44 mg, 0.041 mmol) in trifluoroacetic acid (TFA) (4 mL) was added triethylsilane (0.2 mL), the solution was mixed, and then the solvents were removed under a stream of argon gas. The residue was resolved in a mixed solvent of CH_2Cl_2/MeOH (10 : 1, 22 mL), to which were added $ReOCl_3(PPh_3)_2$ (70 mg, 0.084 mmol) and 1 M AcONa in MeOH (4 mL). The reaction mixture was heated to reflux for 8 h. After cooling to room temperature, $CHCl_3$ (60 mL) was added and filtered. Evaporation of the filtrate gave a residue, which was purified by silica gel chromatography ($CHCl_3$/MeOH = 10 : 1) and then RP-HPLC (MeCN/H_2O = 1 : 1) to give 24 mg of **9** (84%). ^{1}H NMR (400 MHz, DMSO-d_6) δ 9.42 (s, 1H), 8.17 (d, J = 8.8 Hz, 2H), 7.95 (d, J = 8.4 Hz, 1H), 7.49 (dd, J = 8.4, 2.4 Hz, 1H), 7.46 (d, J = 2.4 Hz, 1H), 6.86 (d, J = 8.8 Hz, 2H), 4.30 (t, J = 6.4 Hz, 2H), 4.18–3.83 (m, 4H), 3.64–3.16 (m, 6H), 3.02 (s, 6H), 2.72–1.68 (m, 6H). HRMS (ESI): *m*/*z* calculated for $C_{25}H_{32}N_5NaO_2{}^{187}ReS_2^+$ $[M + Na]^+$, 708.1447; found, 708.1446.

Synthesis of Re-BAT-C3-PQ-2 (10). To a solution of **8** (20 mg, 0.019 mmol) in TFA (8 mL) was added triethylsilane (0.4 mL), the solution was mixed, and then the solvents were removed under a stream of argon gas. The residue was resolved in a mixed solvent of CH_2Cl_2/MeOH (10 : 1, 22 mL), to which were added $ReOCl_3(PPh_3)_2$ (32 mg, 0.038 mmol) and 1 M AcONa in MeOH (4 mL). The reaction mixture was heated to reflux for 2 h.

After cooling to room temperature, H_2O (50 mL) was added. The mixture was extracted with $CHCl_3$ (50 mL × 2) and dried over $MgSO_4$. Evaporation of the solution gave a residue, which was purified by silica gel chromatography ($CHCl_3$/MeOH = 10 : 1) and then RP-HPLC (MeCN/H_2O = 1 : 1) to give 5 mg of **10** (39%). ^{1}H NMR (400 MHz, DMSO-d_6) δ 9.38 (s, 1H), 8.10 (d, J = 8.8 Hz, 2H), 7.93 (d, J = 8.4 Hz, 1H), 7.48 (dd, J = 8.4, 2.4 Hz, 1H), 7.45 (d, J = 2.4 Hz, 1H), 6.69 (d, J = 8.8 Hz, 2H), 4.30 (t, J = 6.4 Hz, 2H), 4.14–3.82 (m, 4H), 3.64–3.17 (m, 6H), 2.76 (s, 3H), 2.72–1.68 (m, 6H). HRMS (ESI): m/z calculated for $C_{24}H_{31}N_5O_2{}^{187}ReS_2{}^+$ $[M + H]^+$, 672.1471; found, 672.1475.

Synthesis of 4-(6-(3-bromopropoxy)quinoxalin-2-yl)aniline (11). To a solution of **6** (49 mg, 0.21 mmol) and 1,3-dibromopropane (84 μL, 0.83 mmol) in MeCN (10 mL) was added K_2CO_3 (85 mg, 0.62 mmol). The mixture was heated to reflux for 2 h. After cooling to room temperature, H_2O (60 mL) was added. The mixture was extracted with AcOEt (60 mL × 2). The organic phases were combined and dried over $MgSO_4$. Evaporation of the solvent afforded a residue, which was purified by silica gel chromatography (AcOEt/hexane = 3 : 1) to give 46 mg of **11** (62%). ^{1}H NMR (400 MHz, $CDCl_3$) δ 9.18 (s, 1H), 8.01 (d, J = 8.4 Hz, 2H), 7.98 (d, J = 10.0 Hz, 1H), 7.42–7.35 (m, 2H), 6.83 (d, J = 8.4 Hz, 2H), 4.28 (t, J = 6.0 Hz, 2H), 3.66 (t, J = 6.4 Hz, 2H), 2.42 (t, J = 6.4 Hz, 2H). MS (ESI): m/z calculated for $C_{18}H_{16}BrN_3O^+$ $[M + H]^+$, 358; found, 358.

Synthesis of *tert*-butyl(2-((3-((2-(4-aminophenyl)quinoxalin-6-yl)oxy)propyl)(2-(tritylthio)ethyl)amino)ethyl)(2-(tritylthio) ethyl)carbamate (12). To a solution of **11** (46 mg, 0.13 mmol) and Trt-Boc-BAT (98 mg, 0.13 mmol) in DMF (15 mL) was added *N*,*N*-diisopropylethylamine (45 μL, 0.26 mmol). The mixture was stirred at 110 °C for 2 h. After cooling to room temperature, H_2O (60 mL) was added. The mixture was extracted with AcOEt/hexane (1 : 1, 60 mL × 2). The organic phases were combined and dried over $MgSO_4$. Evaporation of the solvent afforded a residue, which was purified by silica gel chromatography (AcOEt/hexane = 3 : 1) to give 18 mg of **12** (13%). ^{1}H NMR (400 MHz, $CDCl_3$) δ 9.17 (s, 1H), 8.01 (d, J = 8.4 Hz, 2H), 7.93 (d, J = 9.2 Hz, 1H), 7.41–7.36, (m, 14H), 7.33–7.27 (m, 4H), 7.24–7.15 (m, 12H), 4.15–3.80 (m, 4H), 2.42–2.20 (m, 10H). MS (ESI): m/z calculated for $C_{66}H_{68}N_5O_3S_2{}^+$ $[M + H]^+$, 1043; found, 1043.

Synthesis of Re-BAT-C3-PQ-3 (13). To a solution of **12** (11 mg, 0.011 mmol) in TFA (2 mL) was added triethylsilane (0.1 mL), the solution was mixed, and then the solvents were removed under a stream of argon gas. The residue was resolved in a mixed solvent of CH_2Cl_2/MeOH (10 : 1, 5 mL), to which were added $ReOCl_3(PPh_3)_2$ (18 mg, 0.022 mmol) and 1 M AcONa in MeOH (4 mL). The reaction mixture was heated to reflux overnight. After cooling to room temperature, $CHCl_3$ (60 mL) was added and the mixture was filtered. Evaporation of the filtrate gave a residue, which was purified by silica gel chromatography ($CHCl_3$/MeOH = 9 : 1) and then RP-HPLC (MeCN/H_2O = 1 : 1) to give 4.1 mg of **13** (59%). ^{1}H NMR (400 MHz, DMSO-d_6) δ 9.35 (s, 1H), 8.02 (d, J = 8.8 Hz, 2H), 7.92 (d, J = 8.4 Hz, 1H), 7.47 (d, J = 8.4 Hz, 1H), 7.44 (s, 1H), 6.70 (d, J = 8.8 Hz, 2H), 5.69 (s, 2H), 4.29 (t, J = 5.6 Hz, 2H), 4.18–3.82 (m, 4H), 3.64–3.06 (m, 6H), 2.72–1.68 (m, 6H). HRMS (ESI): m/z calculated for $C_{23}H_{28}N_5NaO_2{}^{187}ReS_2{}^+$ $[M + Na]^+$, 680.1134; found, 680.1134.

^{99m}Tc-labeling reaction

To a solution of sodium glucoheptonate dehydrate (2.0 g, 7.0 mmol) in H_2O (25 mL) was added 0.75 mL of an $SnCl_2 \cdot 2H_2O$ solution [12 mg of tin(II) chloride dehydrate (53 mmol) dissolved in 15 mL of 0.1 M HCl]. This solution was adjusted to pH 8.5–9.0 using a small amount of 0.1 M NaOH. After being lyophilized to give the pulverulent Sn glucoheptonate (SnGH) kit, 1.0 mg of this was weighed and added to an $Na^{99m}TcO_4$ solution (200 μL). The solution was reacted at room temperature for 10 min to give a ^{99m}TcGH solution. A solution of the precursor (**7**, **8**, or **12**) (0.3 mg) in TFA (400 μL) was mixed with triethylsilane (20 μL), and the solvents were removed under a stream of argon gas. The residue was resolved in MeCN (100 μL), followed by the addition of 0.1 M HCl (10 μL) and the ^{99m}TcGH solution (100 μL). The reaction mixture was heated to 110 °C for 20 min. After cooling to room temperature, saturated $NaHCO_3$ (aq.) (30 μL) was added. The mixture was purified by RP-HPLC. The ^{99m}Tc-labeled phenylquinoxaline complex was analyzed by analytical RP-HPLC on a Cosmosil C_{18} column (5C_{18}-AR-II, 4.6 × 150 mm) with a solvent of H_2O/MeCN [11 : 9 (0 min) to 1 : 3 (30 min)] as the mobile phase at a flow rate of 1.0 mL min^{-1}. The radioactivity of the ^{99m}Tc-labeled form was recorded for 30 min.

Measurement of log *P*

The experimental determination of partition coefficients was performed in 1-octanol and phosphate-buffered saline (PBS) (pH 7.4). The two phases were presaturated with each other. 1-Octanol (3.0 mL) and PBS (3.0 mL) were pipetted into a 15 mL test tube containing the ^{99m}Tc complex. The test tube was vortexed for 2 min and centrifuged (5 min, 4000g). Aliquots (500 μL) from the 1-octanol and PBS phases were transferred into two test tubes for counting. One milliliter of the remaining 1-octanol phase, new 1-octanol (2.0 mL), and PBS (3.0 mL) were pipetted into a new test tube. The vortexing, centrifuging, and counting were repeated until consistent partition coefficient values were obtained (usually the sixth partition). The amount of radioactivity in each tube was measured with a γ counter (Wallac 1470 Wizard; PerkinElmer, Massachusetts, U.S.A.). The partition coefficient was calculated using the equation: $\log P = \log[\text{count}_{\text{1-octanol}}/\text{count}_{\text{PBS}}]$.

Binding assay using Aβ(1–42) aggregates in solution

A solid form of Aβ(1–42) was purchased from the Peptide Institute (Osaka, Japan). Aggregation was carried out by gently dissolving the peptide (0.25 mg mL^{-1}) in PBS (pH 7.4). The solution was incubated at 37 °C for 42 h with gentle and constant shaking. Aggregated Aβ(1–42) was used after being diluted to a concentration appropriate for the assays with PBS. The binding assay was performed by mixing 50 μL of Aβ(1–42) aggregates (final conc., 0.125, 1.25, 2.5, and 5.0 μg mL^{-1}), 50 μL of [^{99m}Tc]**14**, [^{99m}Tc]**15**, or [^{99m}Tc]**16** (8.3 kBq in 30% EtOH), and 900 μL of 30% EtOH. After incubation at room temperature for 3 h, the mixture was filtered through Whatman GF/B filters (Whatman, Kent, U.K.) using a Brandel M-24 cell harvester (Brandel, Maryland, U.S.A.), and the radioactivity of the filters

containing the bound ^{99m}Tc complex was measured using a γ counter (PerkinElmer).

Competitive inhibition assay using Aβ(1–42) aggregates in solution

A mixture containing 50 μL of Re complex (**9** or **10**) or 6-iodo-2-(4′-dimethylamino)phenyl-imidazo[1,2-*a*]-pyridine (IMPY) (final conc., 10 pM to 20 μM in DMSO), 50 μL of [^{125}I]IMPY (final conc., 2.5 kBq mL^{-1} in EtOH), 50 μL of Aβ(1–42) aggregates (final conc., 0.125 μg mL^{-1}), and 850 μL of 10% DMSO was incubated at room temperature for 3 h. The mixture was then filtered through Whatman GF/B filters (Whatman) using a Brandel M-24 cell harvester (Brandel), and the radioactivity of the filters containing the bound ^{125}I ligand was measured using a γ counter (PerkinElmer). Values for the half-maximal inhibitory concentration (IC_{50}) were determined from displacement curves of three independent experiments using GraphPad Prism 5.0 (GraphPad Software, Inc., California, U.S.A.), and those for the inhibition constant (K_i) were calculated using the Cheng–Prusoff equation: $K_i = IC_{50}/(1 + [L]/K_d)$,[32] where [L] is the concentration of [^{125}I]IMPY used in the assay and K_d is the dissociation constant of IMPY (4.2 nM).[30]

In vivo biodistribution assessment in normal mice

A saline solution (100 μL) of [^{99m}Tc]**14** (20 kBq) containing EtOH (20 μL) and Tween80 (0.1 mg) was injected directly into the tail vein of ddY mice (male, 5 weeks old). The mice were sacrificed at 2, 10, 30, and 60 min postinjection. The organs of interest were removed and weighed, and radioactivity was measured using a γ counter (PerkinElmer). The % injected dose per g (% ID per g) of samples was calculated by comparing the sample counts with the count of the initial dose.

Ex vivo autoradiography using Tg2576 and wild-type mice

Tg2576 transgenic mice (female, 32 months old) and wild-type mice (female, 32 months old) were used as the AD model and age-matched control, respectively. A saline solution (150 μL) of [^{99m}Tc]**14** (25.9 MBq) containing EtOH (30 μL) and Tween80 (0.15 mg) was injected through the tail vein. After the mice were sacrificed at 30 min postinjection by decapitation, the brain was immediately removed, embedded in Super Cryoembedding Medium (SCEM) compound (SECTION-LAB Co., Ltd., Hiroshima, Japan), and then frozen in a dry ice/hexane bath. Frozen sections were prepared at a 30 μm thickness and exposed to a BAS imaging plate (Fuji Film, Tokyo, Japan) overnight. Autoradiographic images were obtained using a BAS5000 scanner system (Fuji Film). After autoradiographic examination, the same sections were stained by thioflavin-S to confirm the presence of Aβ depositions. For thioflavin-S fluorescent staining, the sections were immersed in a 100 μM thioflavin-S solution containing 50% EtOH for 3 min, washed in 50% EtOH for 1 min two times, and examined using a microscope (BIOREVO BZ-9000; Keyence Corp., Osaka, Japan) equipped with a GFP-BP filter set.

Results and discussion

Chemistry

The synthesis of the precursors for the ^{99m}Tc-labeling and the corresponding Re complex based on phenylquinoxaline is outlined in Scheme 1. A methoxy group of 6-methoxy-2-chloroquinoxaline was converted to a hydroxyl group using $AlCl_3$/toluene according to our previous report,[30] which afforded **3**. The phenylquinoxaline backbone was formed by the Suzuki coupling reaction between **3** and the corresponding boronate ester, which afforded **4**, **5**, and **6** in 89, 61, and 10% yields, respectively. The thiol-protected chelation ligand (Trt-Boc-BAT) was synthesized as reported previously.[21] A trimethylene group was introduced into Trt-Boc-BAT and **6** as a linker by reacting them with 1,3-dibromopropane, which afforded **2** and **11** in 26 and 62% yields, respectively.[24] The precursors for ^{99m}Tc-labeling, compounds **7**, **8**, and **12**, were synthesized by conjugating the chelating ligand and phenylquinoxaline scaffold.[24] Technetium has no stable isotopes; therefore, direct structural characterization is very challenging. Since rhenium, the group VIIB congener of technetium, generally produces complexes with similar physical and biological properties to those of technetium, it is often used as a nonradioactive surrogate of technetium for large-scale synthesis and structural characterization.[19,21,22,24–27] We prepared the corresponding Re complexes with phenylquinoxaline. After deprotection of the thiol groups of **7**, **8**, and **12** in TFA and triethylsilane, the Re complexes **9** (Re-BAT-C3-PQ-1), **10** (Re-BAT-C3-PQ-2), and **13** (Re-BAT-C3-PQ-3) were synthesized, respectively, through a reaction with $ReOCl_3(PPh_3)_2$. ^{1}H NMR spectra and the HPLC profiles for three Re complexes (**9**, **10**, and **13**) proved their high-level purity (ESI Fig. S1–S4†).

^{99m}Tc-labeling reaction

The ^{99m}Tc-labeling reaction was performed by a ligand exchange reaction employing the precursors **7**, **8**, and **12** with ^{99m}TcGH, which afforded [^{99m}Tc]**14** (^{99m}Tc-BAT-C3-PQ-1), [^{99m}Tc]**15** (^{99m}Tc-BAT-C3-PQ-2), and [^{99m}Tc]**16** (^{99m}Tc-BAT-C3-PQ-3), respectively (Scheme 2). The radiochemical yields for [^{99m}Tc]**14**, [^{99m}Tc]**15**, and [^{99m}Tc]**16** were 56, 62, and 44%, respectively. The resulting mixture was analyzed by RP-HPLC, showing that a single radioactive complex was formed with radiochemical purity higher than 99% after purification by HPLC. The radiochemical identity of the ^{99m}Tc complex was verified by comparative HPLC using the corresponding Re complex as a reference (Table 1). The retention times on RP-HPLC (radioactivity) for [^{99m}Tc]**14** (^{99m}Tc-BAT-C3-PQ-1), [^{99m}Tc]**15** (^{99m}Tc-BAT-C3-PQ-2), and [^{99m}Tc]**16** (^{99m}Tc-BAT-C3-PQ-3) were 23.3, 16.6, and 10.8 min, respectively. Moreover, the retention times on RP-HPLC (absorption at 254 nm) for **9** (Re-BAT-C3-PQ-1), **10** (Re-BAT-C3-PQ-2), and **13** (Re-BAT-C3-PQ-3) were 22.1, 15.6 and 10.1 min, respectively. The retention times between ^{99m}Tc-labeled tracers and the corresponding Re complexes suggest that the desired ^{99m}Tc-labeled phenylquinoxaline derivatives were successfully synthesized.

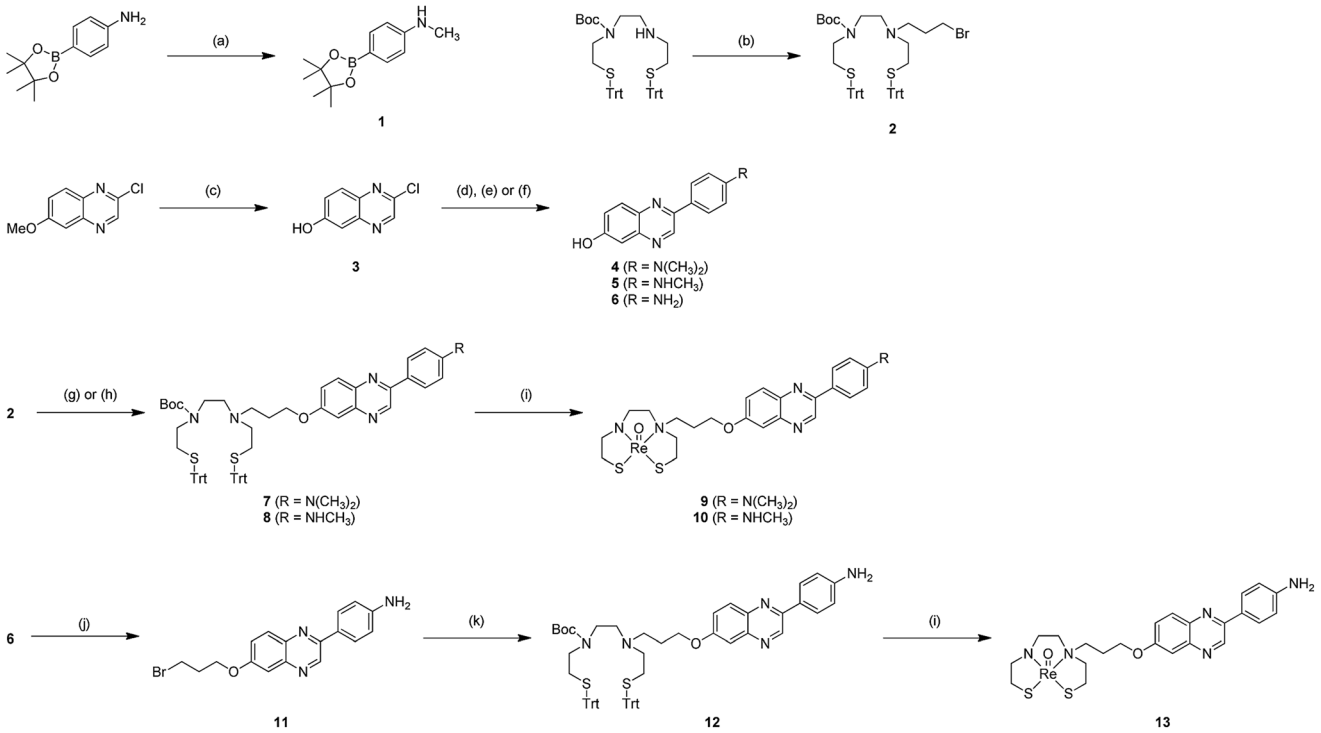

Scheme 1 Synthetic route for phenylquinoxaline derivatives. Reagents and conditions: (a) (1) paraformaldehyde, sodium methoxide, MeOH, reflux, (2) $NaBH_4$, reflux; (b) 1,3-dibromopropane, *N*,*N*-diisopropylethylamine, DMF, 90 °C; (c) $AlCl_3$, toluene, 0 °C to 80 °C; (d) *N*,*N*-dimethyl-4-(4,4,5,5-tetramethyl-1,3,2-dioxaborolan-2-yl)aniline, $Pd(PPh_3)_4$, dioxane, 2 M Na_2CO_3 (aq.), reflux; (e) **1**, $Pd(PPh_3)_4$, dioxane, 2 M Na_2CO_3 (aq.), reflux; (f) 4-(4,4,5,5-tetramethyl-1,3,2-dioxaborolan-2-yl)aniline, $Pd(PPh_3)_4$, dioxane, 2 M Na_2CO_3 (aq.), reflux; (g) **4**, Cs_2CO_3, DMF, 70 °C; (h) **5**, Cs_2CO_3, DMF, 70 °C; (i) (1) triethylsilane, TFA, room temperature, (2) $ReOCl_3(PPh_3)_2$, AcONa, CH_2Cl_2, MeOH, reflux; (j) 1,3-dibromopropane, K_2CO_3, MeCN, reflux; (k) Trt-Boc-BAT, *N*,*N*-diisopropylethylamine, DMF, 110 °C.

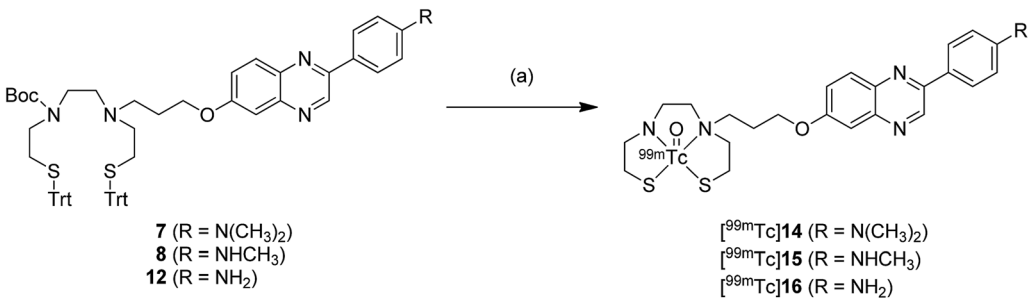

Scheme 2 ^{99m}Tc-labeling of phenylquinoxaline derivatives. Reagents and conditions: (a) (1) triethylsilane, TFA, room temperature, (2) ^{99m}Tc-glucoheptonate, 0.1 N HCl, MeCN, 110 °C.

Binding assay using Aβ(1–42) aggregates in solution

To evaluate the binding affinity for Aβ(1–42) aggregates of [^{99m}Tc]**14** (^{99m}Tc-BAT-C3-PQ-1), [^{99m}Tc]**15** (^{99m}Tc-BAT-C3-PQ-2), and [^{99m}Tc]**16** (^{99m}Tc-BAT-C3-PQ-3), an *in vitro* binding experiment in solution was carried out. Fig. 2 shows the binding affinity of [^{99m}Tc]**14**, [^{99m}Tc]**15**, and [^{99m}Tc]**16** as specific Aβ(1–42) aggregate-bound radioactivity (%) at different concentrations of Aβ(1–42) aggregates. The percent radioactivity of [^{99m}Tc]**14** (^{99m}Tc-BAT-C3-PQ-1) and [^{99m}Tc]**15** (^{99m}Tc-BAT-C3-PQ-2) bound to aggregates increased dependent on the dose of Aβ(1–42), while [^{99m}Tc]**16** (^{99m}Tc-BAT-C3-PQ-3) showed no marked affinity for the aggregates. In terms of Aβ(1–42) aggregate-bound radioactivity, the derivatives ranked in the following order: [^{99m}Tc]**14** > [^{99m}Tc]**15** > [^{99m}Tc]**16**, at all concentrations of Aβ(1–42) aggregates. The order in terms of the strength of binding corresponded with those of radioiodinated

Table 1 HPLC retention times of ^{99m}Tc/Re complexes[a]

Re complex	Retention time	^{99m}Tc complex	Retention time
9	22.1 min	[^{99m}Tc]**14**	23.3 min
10	15.6 min	[^{99m}Tc]**15**	16.6 min
13	10.1 min	[^{99m}Tc]**16**	10.8 min

[a] RP-HPLC using a solution of H_2O/MeCN [11 : 9 (0 min) to 1 : 3 (30 min)] as a mobile phase.

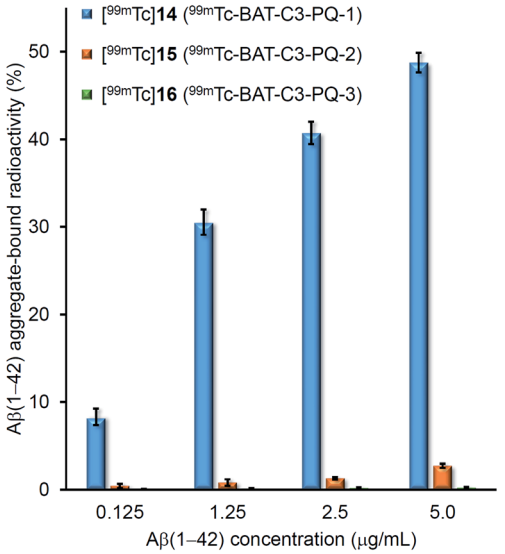

Fig. 2 Binding assay of ^{99m}Tc-labeled phenylquinoxaline derivatives using Aβ(1–42) aggregates. Values are the mean ± standard deviation of the mean of three independent experiments.

and radiofluorinated quinoxaline derivatives; in other words, the affinity increased in the order of the *N*,*N*-dimethylated derivative > *N*-monomethylated derivative > primary amino derivative.[29,30]

Competitive inhibition assay using Aβ(1–42) aggregates in solution

Since [^{99m}Tc]**14** and [^{99m}Tc]**15** showed affinity for Aβ aggregates in the Aβ(1–42) binding assay, quantitative binding affinity for Aβ aggregates was evaluated with rhenium complexes **9** (Re-BAT-C3-PQ-1) and **10** (Re-BAT-C3-PQ-2) according to conventional methods using [^{125}I]IMPY.[33] Both Re complexes **9** and **10** inhibited the binding of [^{125}I]IMPY in a dose-dependent manner, with K_i values of 53.7 and 296 nM, respectively (Table 2). The affinity for Aβ(1–42) aggregates of Re complexes well reflected that of the corresponding ^{99m}Tc complexes, confirmed above. These Re complexes showed the K_i values, which were comparable to those of the corresponding Re complexes of the ^{99m}Tc-labeled probes reported previously (13.6–393 nM).[24,26,27] The binding affinity of the *N*,*N*-dimethylated derivative (**9**) was slightly lower than that of PIB (9.00 nM)[34] and IMPY (12.3 nM), indicating that it may exhibit sufficient affinity for the imaging of Aβ(1–42) aggregates *in vivo*.

Table 2 Inhibition constants (K_i, nM) for the binding of Re complexes and IMPY to Aβ(1–42) aggregates determined using [^{125}I]IMPY as ligand

Compound	K_i[a] (nM)
9 (Re-BAT-C3-PQ-1)	53.7 ± 8.77
10 (Re-BAT-C3-PQ-2)	296 ± 26.0
IMPY	12.3 ± 1.52

[a] Values are the mean ± standard error of the mean for six independent experiments.

However, the K_i values of these Re complexes were higher than those of quinoxaline derivatives with introduced iodine (4.1 nM) and fluorine (0.895 nM) reported previously.[29,30] This result suggests that the introduction of the bulky ^{99m}Tc-BAT complex into the phenylquinoxaline scaffold interferes with the binding to Aβ(1–42) aggregates, as shown in some reports on other Aβ imaging probes conjugated with the ^{99m}Tc-BAT complex.[24] According to the result of binding affinity for Aβ(1–42) aggregates *in vitro*, further studies were conducted using [^{99m}Tc]**14** (^{99m}Tc-BAT-C3-PQ-1) with the highest binding affinity.

In vivo biodistribution assessment in normal mice

To evaluate the brain uptake of [^{99m}Tc]**14** (^{99m}Tc-BAT-C3-PQ-1), a biodistribution experiment was performed with normal mice (Table 3). An ideal Aβ imaging probe should show high-level efficiency along with BBB penetration to deliver an adequate dose into the brain, and then achieve rapid clearance of the non-bound tracer from the brain to reduce the background signal in the AD brain. Previous studies suggested that the optimal measured log *P*-value of compounds to pass freely across the BBB ranged from 0.9 to 2.5.[35] The log *P*-value for [^{99m}Tc]**14** was 2.45, indicating that this complex might penetrate the BBB. [^{99m}Tc]**14** showed the highest initial uptake at 2 min postinjection (0.88% ID per g), which was comparable or slightly lower than those of ^{99m}Tc-labeled probes reported previously (0.2–1.80% ID per g).[19–22,24–27] The radioactivity of [^{99m}Tc]**14** in the brain was rapidly eliminated (0.25% ID per g at 60 min postinjection). The $\text{brain}_{2\ \text{min}}/\text{brain}_{60\ \text{min}}$ ratio is generally used as an index for evaluating pharmacokinetics *in vivo*. The $\text{brain}_{2\ \text{min}}/\text{brain}_{60\ \text{min}}$ ratio of ^{99m}Tc-BAT-C3-PQ-1 was 3.52, indicating that it displayed one of the best profiles of radioactivity in the brain among ^{99m}Tc complexes reported previously.[19–22,24–27] Although the $\text{brain}_{2\ \text{min}}/\text{brain}_{60\ \text{min}}$ ratio of ^{99m}Tc-BAT-C3-PQ-1 was lower than those of [^{11}C]PIB (11.7)[6] and [^{123}I]IMPY (14.4),[33] it was comparable to that of [^{18}F]florbetapir (3.80).[30] These indicate its promising property for the imaging

Table 3 Biodistribution of radioactivity after intravenous injection of [^{99m}Tc]**14** (^{99m}Tc-BAT-C3-PQ-1) in normal mice[a]

	Time after injection (min)			
Tissue	2	10	30	60
Blood	10.97 (0.90)	5.39 (0.32)	3.04 (0.20)	2.38 (0.17)
Liver	27.07 (0.60)	29.66 (1.96)	31.41 (1.63)	26.25 (1.47)
Kidney	12.51 (1.18)	9.12 (0.33)	6.47 (0.36)	4.84 (0.58)
Intestine	2.35 (0.33)	6.06 (0.48)	14.22 (1.96)	16.88 (2.92)
Spleen	4.53 (1.23)	3.32 (0.19)	2.38 (0.26)	1.84 (0.25)
Pancreas	4.92 (0.22)	3.95 (0.51)	2.82 (0.19)	2.09 (0.93)
Heart	10.40 (1.00)	4.17 (0.25)	2.64 (0.18)	1.88 (0.21)
Lung	12.72 (1.12)	6.82 (0.50)	4.97 (0.56)	3.38 (0.57)
Stomach[b]	1.90 (0.17)	4.89 (1.31)	8.44 (1.90)	6.79 (0.82)
Brain	0.88 (0.08)	0.77 (0.08)	0.52 (0.03)	0.25 (0.02)

[a] Expressed as % injected dose per gram of tissue. Each value is the mean (standard deviation) of five animals at each interval. [b] Expressed as % injected dose.

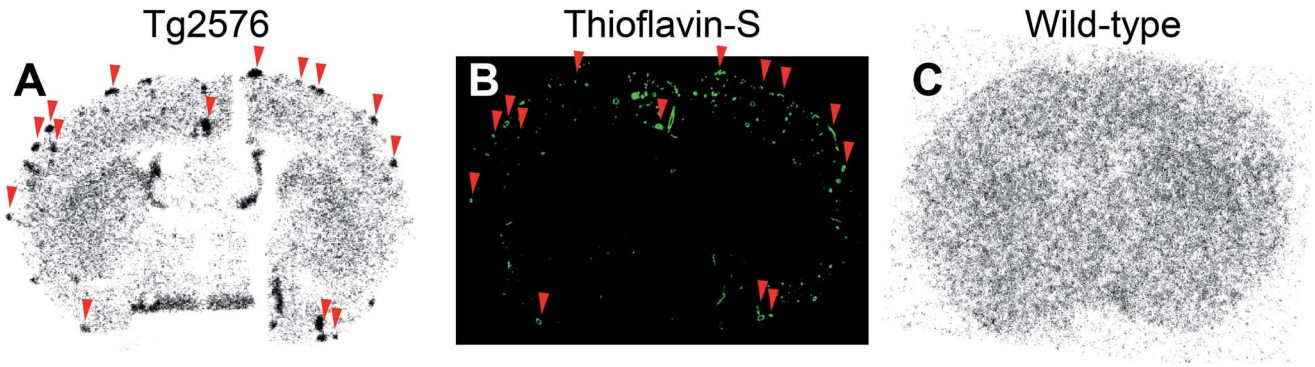

Fig. 3 *Ex vivo* autoradiograms from a Tg2576 mouse (A) and a wild-type mouse (C) with [^{99m}Tc]**14** (^{99m}Tc-BAT-C3-PQ-1). The same sections are also stained with thioflavin-S (B).

of Aβ in the brain. Unfortunately, radioactivity in the stomach suggests the partial decomposition to pertechnetate *in vivo*.

Ex vivo autoradiography using Tg2576 and wild-type mice

According to the results of the binding affinity assay *in vitro* and biodistribution in normal mice, we further evaluated the potential of [^{99m}Tc]**14** (^{99m}Tc-BAT-C3-PQ-1) for imaging Aβ plaques in the AD model mouse. An *ex vivo* autoradiographic examination was carried out using Tg2576 transgenic mouse (Fig. 3). Since Tg2576 mice are known to overproduce Aβ aggregates in the brain, they have been commonly used to evaluate the specific binding to Aβ aggregates in experiments *in vitro* and *in vivo*.[24,30,36] The brain was removed at 30 min post-injection for autoradiography. [^{99m}Tc]**14** showed intensive radioactive spots in sections from the Tg2576 mouse, but not the age-matched control (Fig. 3A and C). Furthermore, these spots corresponded with Aβ depositions confirmed by fluorescent staining in the same sections with thioflavin-S, a histochemical dye commonly used to stain Aβ plaques (Fig. 3B, red arrowheads). This suggests that ^{99m}Tc-BAT-C3-PQ-1 had sufficient properties to detect Aβ plaques in the transgenic mouse, although it displayed a lower affinity for Aβ aggregates and lower brain uptake in normal mice than the clinically utilized probes, such as [^{11}C]PIB and [^{18}F]florbetapir. In addition, the nonspecific accumulation of radioactivity within the white matter, which was demonstrated in our previous reports,[30] was not observed for ^{99m}Tc-BAT-C3-PQ-1, as shown in Fig. 3A and C, probably due to its low brain uptake. However, some Aβ depositions were not labeled with ^{99m}Tc-BAT-C3-PQ-1. This may derive from its low brain uptake, low affinity, and low *in vivo* stability, which are insufficient to bind to Aβ aggregates deposited in the whole brain. Therefore, further modifications are required to improve the properties of ^{99m}Tc-labeled phenylquinoxaline derivatives for imaging Aβ plaques in AD brains.

Conclusion

We successfully synthesized three ^{99m}Tc-labeled phenylquinoxaline derivatives and their corresponding Re complexes. Among them, ^{99m}Tc-BAT-C3-PQ-1 and its corresponding Re complex showed sufficient binding affinity for Aβ aggregates in an *in vitro* binding assay. An *in vivo* biodistribution study with ^{99m}Tc-BAT-C3-PQ-1 in normal mice indicated its moderate initial brain uptake and reasonable clearance from the brain. Moreover, it showed extensive labeling of Aβ plaques in the transgenic mouse brain. Taken together, the findings in the present study provide important information on developing clinically useful ^{99m}Tc-labeled Aβ imaging probes for the diagnosis of AD based on quinoxaline derivatives. Additional modifications to further improve the pharmacokinetics in the brain and the binding affinity for Aβ aggregates of ^{99m}Tc complexes are underway.

Acknowledgements

The study was supported by a Grant-in-Aid for Scientific Research (B) (Grant Number 26293274), the Nakatani Foundation for Advancement of Measuring Technologies in Biomedical Engineering, Japan Research Foundation for Clinical Pharmacology, and a JSPS Research Fellowship for Young Scientists (16J05493).

References

1 A. Nordberg, *Lancet Neurol.*, 2004, **3**, 519–527.
2 R. L. Nussbaum and C. E. Ellis, *N. Engl. J. Med.*, 2003, **348**, 1356–1364.
3 E. Giacobini and R. E. Becker, *J. Alzheimer's Dis.*, 2007, **12**, 37–52.
4 S. Hatashita, H. Yamasaki, Y. Suzuki, K. Tanaka, D. Wakebe and H. Hayakawa, *Eur. J. Nucl. Med. Mol. Imaging*, 2014, **41**, 290–300.
5 W. E. Klunk, H. Engler, A. Nordberg, Y. Wang, G. Blomqvist, D. P. Holt, M. Bergstrom, I. Savitcheva, G. F. Huang, S. Estrada, B. Ausen, M. L. Debnath, J. Barletta, J. C. Price, J. Sandell, B. J. Lopresti, A. Wall, P. Koivisto, G. Antoni, C. A. Mathis and B. Langstrom, *Ann. Neurol.*, 2004, **55**, 306–319.
6 C. A. Mathis, Y. Wang, D. P. Holt, G. F. Huang, M. L. Debnath and W. E. Klunk, *J. Med. Chem.*, 2003, **46**, 2740–2754.
7 R. Ni, P. G. Gillberg, A. Bergfors, A. Marutle and A. Nordberg, *Brain*, 2013, **136**, 2217–2227.

8 K. J. Lin, W. C. Hsu, I. T. Hsiao, S. P. Wey, L. W. Jin, D. Skovronsky, Y. Y. Wai, H. P. Chang, C. W. Lo, C. H. Yao, T. C. Yen and M. P. Kung, *Nucl. Med. Biol.*, 2010, **37**, 497–508.

9 D. F. Wong, P. B. Rosenberg, Y. Zhou, A. Kumar, V. Raymont, H. T. Ravert, R. F. Dannals, A. Nandi, J. R. Brasic, W. Ye, J. Hilton, C. Lyketsos, H. F. Kung, A. D. Joshi, D. M. Skovronsky and M. J. Pontecorvo, *J. Nucl. Med.*, 2010, **51**, 913–920.

10 R. Lundqvist, J. Lilja, B. A. Thomas, J. Lotjonen, V. L. Villemagne, C. C. Rowe and L. Thurfjell, *J. Nucl. Med.*, 2013, **54**, 1472–1478.

11 N. Nelissen, K. Van Laere, L. Thurfjell, R. Owenius, M. Vandenbulcke, M. Koole, G. Bormans, D. J. Brooks and R. Vandenberghe, *J. Nucl. Med.*, 2009, **50**, 1251–1259.

12 G. A. Becker, M. Ichise, H. Barthel, J. Luthardt, M. Patt, A. Seese, M. Schultze-Mosgau, B. Rohde, H. J. Gertz, C. Reininger and O. Sabri, *J. Nucl. Med.*, 2013, **54**, 723–731.

13 W. Zhang, S. Oya, M. P. Kung, C. Hou, D. L. Maier and H. F. Kung, *Nucl. Med. Biol.*, 2005, **32**, 799–809.

14 H. F. Kung, M. P. Kung, Z. P. Zhuang, C. Hou, C. W. Lee, K. Plössl, B. Zhuang, D. M. Skovronsky, V. M. Lee and J. Q. Trojanowski, *Mol. Imaging Biol.*, 2003, **5**, 418–426.

15 W. Qu, M. P. Kung, C. Hou, T. E. Benedum and H. F. Kung, *J. Med. Chem.*, 2007, **50**, 2157–2165.

16 M. Ono, Y. Cheng, H. Kimura, H. Watanabe, K. Matsumura, M. Yoshimura, S. Iikuni, Y. Okamoto, M. Ihara, R. Takahashi and H. Saji, *PLoS One*, 2013, **8**, e74104.

17 C. J. Chen, K. Bando, H. Ashino, K. Taguchi, H. Shiraishi, K. Shima, O. Fujimoto, C. Kitamura, S. Matsushima, K. Uchida, Y. Nakahara, H. Kasahara, T. Minamizawa, C. Jiang, M. R. Zhang, M. Ono, M. Tokunaga, T. Suhara, M. Higuchi, K. Yamada and B. Ji, *J. Nucl. Med.*, 2015, **56**, 120–126.

18 Y. Maya, Y. Okumura, R. Kobayashi, T. Onishi, Y. Shoyama, O. Barret, D. Alagille, D. Jennings, K. Marek, J. Seibyl, G. Tamagnan, A. Tanaka and Y. Shirakami, *Brain*, 2016, **139**, 193–203.

19 Z. P. Zhuang, M. P. Kung, C. Hou, K. Ploessl and H. F. Kung, *Nucl. Med. Biol.*, 2005, **32**, 171–184.

20 K. Serdons, T. Verduyckt, J. Cleynhens, C. Terwinghe, L. Mortelmans, G. Bormans and A. Verbruggen, *Bioorg. Med. Chem. Lett.*, 2007, **17**, 6086–6090.

21 M. Ono, R. Ikeoka, H. Watanabe, H. Kimura, T. Fuchigami, M. Haratake, H. Saji and M. Nakayama, *ACS Chem. Neurosci.*, 2010, **1**, 598–607.

22 M. Ono, R. Ikeoka, H. Watanabe, H. Kimura, T. Fuchigami, M. Haratake, H. Saji and M. Nakayama, *Bioorg. Med. Chem. Lett.*, 2010, **20**, 5743–5748.

23 M. Sagnou, D. Benaki, C. Triantis, T. Tsotakos, V. Psycharis, C. P. Raptopoulou, I. Pirmettis, M. Papadopoulos and M. Pelecanou, *Inorg. Chem.*, 2011, **50**, 1295–1303.

24 Y. Cheng, M. Ono, H. Kimura, M. Ueda and H. Saji, *J. Med. Chem.*, 2012, **55**, 2279–2286.

25 M. Ono, Y. Fuchi, T. Fuchigami, N. Kobashi, H. Kimura, M. Haratake, H. Saji and M. Nakayama, *ACS Med. Chem. Lett.*, 2010, **1**, 443–447.

26 Y. Yang, M. Cui, B. Jin, X. Wang, Z. Li, P. Yu, J. Jia, H. Fu, H. Jia and B. Liu, *Eur. J. Med. Chem.*, 2013, **64**, 90–98.

27 X. Wang, M. Cui, J. Jia and B. Liu, *Eur. J. Med. Chem.*, 2015, **89**, 331–339.

28 X. Wang, M. Cui, P. Yu, Z. Li, Y. Yang, H. Jia and B. Liu, *Bioorg. Med. Chem. Lett.*, 2012, **22**, 4327–4331.

29 M. Cui, M. Ono, H. Kimura, B. Liu and H. Saji, *Bioorg. Med. Chem. Lett.*, 2011, **21**, 4193–4196.

30 M. Yoshimura, M. Ono, K. Matsumura, H. Watanabe, H. Kimura, M. Cui, Y. Nakamoto, K. Togashi, Y. Okamoto, M. Ihara, R. Takahashi and H. Saji, *ACS Med. Chem. Lett.*, 2013, **4**, 596–600.

31 P. Yu, M. Cui, X. Wang, X. Zhang, Z. Li, Y. Yang, J. Jia, J. Zhang, M. Ono, H. Saji, H. Jia and B. Liu, *Eur. J. Med. Chem.*, 2012, **57**, 51–58.

32 Y. Cheng and W. H. Prusoff, *Biochem. Pharmacol.*, 1973, **22**, 3099–3108.

33 M. P. Kung, C. Hou, Z. P. Zhuang, B. Zhang, D. Skovronsky, J. Q. Trojanowski, V. M. Lee and H. F. Kung, *Brain Res.*, 2002, **956**, 202–210.

34 M. Ono, Y. Cheng, H. Kimura, M. Cui, S. Kagawa, R. Nishii and H. Saji, *J. Med. Chem.*, 2011, **54**, 2971–2979.

35 D. D. Dishino, M. J. Welch, M. R. Kilbourn and M. E. Raichle, *J. Nucl. Med.*, 1983, **24**, 1030–1038.

36 A. Alpar, U. Ueberham, M. K. Bruckner, G. Seeger, T. Arendt and U. Gartner, *Brain Res.*, 2006, **1099**, 189–198.